Hexabromocyclododecanes Are Dehalogenated by CYP168A1 from Pseudomonas aeruginosa Strain HS9

Hexabromocyclododecanes are dehalogenated by CYP168A1 from a *Pseudomonas* strain HS9

Ling Huang[1†], Weiwei Wang[1†], Giulio Zanaroli[2], Ping Xu[1] and Hongzhi Tang[1*]

[1]State Key Laboratory of Microbial Metabolism, and School of Life Sciences & Biotechnology, Shanghai Jiao Tong University, Shanghai 200240, People's Republic of China

[2]Department of Civil, Chemical, Environmental and Materials Engineering (DICAM), University of Bologna, Bologna 40131, Italy

†These authors contributed equally to this study.

*Corresponding author: H. Z. Tang; Mailing address: School of Life Sciences & Biotechnology, Shanghai Jiao Tong University, Shanghai 200240, P. R. China;

E-mail: tanghongzhi@sjtu.edu.cn; Tel: +86-21-34204066; Fax: +86-21-34206723.

Abstract

Hexabromocyclododecanes (HBCDs) are widely used brominated flame retardants, which cause antidiuretic hormone syndrome and even induce cancer. However, little information is available about the degrading mechanisms of HBCDs. In this study, genomic, proteomic analyses, RT-qPCR and gene knockout assays reveal that a cytochrome P450 encoding gene is responsible for the HBCD catabolism in *Pseudomonas aeruginosa* HS9. CO-difference spectrum of the enzyme CYP168A1 was matched to P450 character and proved by western blot analysis and UV-visible. We demonstrate that the reactions of debromination and hydrogenation are carried out one after another based on detection of the metabolites pentabromocyclododecanols (PBCDOHs), tetrabromocyclododecadiols (TBCDDOHs) and Br^- iron. In the ^{18}O isotope experiments, PBCD^{18}OHs were only detected in the $H_2{}^{18}O$ group, proving that the added oxygen is derived from H_2O not from O_2. This study elucidates the degrading mechanism of HBCDs by *Pseudomonas*.

Importance

Hexabromocyclododecanes (HBCDs) are environmental pollutants, which are wildly used in industry. In this study, we identified and characterized a novel key dehalogenase CYP168A1 responsible for the HBCDs degradation from a *Pseudomonas aeruginosa* strain HS9. This study provides new insights into understanding biodegradation of HBCDs.

Introduction

Hexabromocyclododecanes (HBCDs) are the second most widely used brominated flame retardants (BFRs), and are utilized in building materials, electronics, textiles, and plastics (1). They are a threat to human health due to causing antidiuretic hormone syndrome and even inducing cancer. Microorganisms play important roles in degradation and detoxification of pollutants of HBCDs (2). However, little information is available about molecular and biochemical mechanisms, particularly how functional proteins relate to debromination. Only two dehalogenases, LinA and LinB from the hexachlorocyclohexane transformation strain *Sphingobium indicum* B90A, can convert HBCD to different debrominated products. LinA selectively catalyzes the transformation of *β*-HBCDs to *1E,5S,6S,9R,10S*-pentabromocyclododecene (PBCDE), while LinB transforms all *α-, β-,* and *γ*-HBCD isomers to pentabromocyclododecanols (PBCDOHs) and even tetrabromocyclododecadiols (TBCDDOHs) (3-4). The kinetics and stereochemistry of LinB-catalyzed *γ*-HBCD transformation have been described in detail, with *Km*, *kcat*, and *kcat*/*Km* values at 1.82 ± 0.60 μmol/L, 0.25 ± 0.10 μmol/L/h and 13.0 ± 6.2 L/mol/s. The results suggest that LinB has a high capability to dehalogenate *γ*-HBCD (5).

Catalytic enzyme resources from bacteria are abundant, and cytochrome P450 enzymes (CYPs) are the key enzymes responsible for the degradation of numerous endogenous compounds. CYPs are involved in the degradation and detoxification of multiple toxicants, such as herbicides, xenobiotic poly aromatic hydrocarbons,

halogenated aromatics, and polychlorinated biphenyls (6-10). Hydroxylation is the typical metabolic reaction of xenobiotics catalyzed by CYPs. Transformed CYP81As from *Echinochloa phyllopogon* decreased—the susceptibility of *Arabidopsis* to clomazone (11-12). Mammalian CYPs (CYP1 family) degrade dibenzo-*p*-dioxins (PCDDs) with efficient activity, and the rat CYP1A1 family also showed high activity towards 2,3,7-trichloro-dibenzo-*p*-dioxin, with the detection of hydroxylated products, 8-hydroxy-2,3,7-trichloro-dibenzo-*p*-dioxins (13). CYP101 dehalogenates hexachlorobenzene with a different metabolic method, in which the halogen atoms are replaced by hydroxyl groups (14). CYP2E1 from *Nicotiana tabacum*, CYP3A4 from human liver and CYPs (CYP71C3v2, CYP71C1, CYP81A1 and CYP97A16) from maize can metabolize HBCDs, and the hydroxylated metabolites OH-HBCDs, OH-PBCDs and OH-TBCDs have been detected (15-20). However, the substitution reaction of HBCDs by CYPs is rarely reported.

Previous work by our research group on *Pseudomonas aeruginosa* HS9 indicated that HBCDs could be degraded to PBCDOHs. Strain HS9 was reported to be a HBCD-metabolizing bacterium based on its ability to convert HBCDs to PBCDOHs or tetrabromocyclododecene (TBCDe), dibromocyclododecadiene (DBCDi), and cyclododecatriene (CDT) (21). In this study, the whole-genome sequence of strain HS9 was sequenced and analyzed, and putative genes for HBCD degradation were elucidated. By combining metabolite analysis with real-time fluorescence quantification experiments (RT-qPCR), the cytochrome P450 enzyme CYP168A1 was considered as the initial dehalogenase in HBCD metabolism. The gene *cyp168A1* was

cloned and expressed in *Escherichia coli*. The subsequent enzymatic properties were investigated on the purified CYP168A1.

Materials and methods

Chemicals. 1, 2, 5, 6, 9, 10-Hexabromocyclododecanes (HBCDs, ≥ 95%) were purchased from Anpel (New Jersey, USA). Hexachlorobenzene (HCB, ≥ 95%) was purchased from AccuStandard (Connecticut, USA). Ethyl acetate, methanol, and all the other regents and solvents used in this study were of analytical grade.

Strains and culture media. *Pseudomonas aeruginosa* HS9 was isolated by our research group in previous work, and it can be obtained from the China Center for Type Culture Collection (CCTCC) under accession M 2019094 (20). *Escherichia coli* DH5*α* and BL21(DE3) (Novagen, Inc. USA) were used for plasmid construction and protein expression, respectively. Lysogeny broth (LB), containing 5 g/L yeast extraction, 10 g/L tryptone and 5 g/L NaCl, or LB agar (1.5% wt/vol) plates with appropriate antibiotics were used to culture *E. coli* (22). *E. coli* harboring each of the constructed plasmids was grown at 37°C, 200 rpm with 50 mg/L kanamycin or 100 mg/L ampicillin for pET28a or pETduet-1 vectors. Strain HS9 was grown at 30°C in mineral salt medium (MSM) containing 5.0 g/L K_2HPO_4, 3.7 g/L KH_2PO_4, 1.0 g/L Na_2SO_4, 0.2 g/L $MgSO_4 \cdot 7H_2O$, 2.0 g/L NH_4Cl and 0.5 mL 2,000-times trace elements solution. The trace elements solution consisted of 0.3 g/L $FeCl_2 \cdot 4H_2O$, 0.038 g/L $CaCl_2 \cdot 6H_2O$, 0.02 g/L $MnCl_2 \cdot 4H_2O$, 0.014 g/L $ZnCl_2$, 0.0124 g/L H_3BO_3, 0.04 g/L

$Na_2MoO_4 \cdot 2H_2O$ and 0.0034 g/L $CuCl_2 \cdot 2H_2O$ (21).

Genome sequencing and proteomic assay of strain HS9. The genomic DNA of strain HS9 was extracted using a Wizard genomic purification kit A1125 (Promega, USA). Genome sequencing was performed on the Illumina Hiseq-2000 platform. Functional genes were predicted and annotated with the Rapid Annotations using Subsystems Technology (RAST) annotation server (23). This whole genome sequence project was submitted to GenBank under accession GCA_003319235.1. Proteomic analysis comparing the protein expression of cells incubated in the presence or absence of 1 mg/L HBCDs MSM media was carried out as follows. Strain HS9 was cultured in 2 L flasks containing 1 L HBCDs-MSM. As a control group, strain HS9 was grown in sodium citrate medium. A total of 10 L of culture were collected during the exponential phase. Both groups were detected with three biological replicates (22).

Quantitative RT-qPCR. Total RNA was isolated from strain HS9 incubated in the presence or absence of 1 mg/L HBCD MSM media, using a total RNA kit (Tiangen, China). Total cDNA was synthesized using a SuperScript III reverse transcriptase (Invitrogen, USA). The 20 μL reverse transcription reaction system contained 1.0 μg total RNA, 0.5 mM dNTP mix, 200 U transcriptase, and 12.5 ng random primers. The reactions were performed according to the manufacturer's protocols. RT-qPCR was then carried out using the CEX96 real-time PCR detection system (Bio-Rad) with a SYBR green I Real Master Mix (TianGen, China). All the data of candidate genes was

normalized to the expression level of 16S rRNA and presented as relative to the expression level in cells growing in the absence of HBCDs. All detections were performed with three replicates (23−25).

Expression and purification of heterologous expressed His-CYP168A1. The DNA fragment of *cyp168A1* was amplified by pfu DNA polymerase (New England Biolabs, Ipswich, MA) with primers Fcyp168A1 (CCGGAATTCCTACTCGCAGGTCTTCTGAG) and Rcyp168A1 (CCCAAGCTTATGGACGACGCATTCAGCGA), in which the enzyme digestion sites (*Eco*RI and *Hin*dIII) are underlined. The double enzyme digested DNA fragments were ligated into expression vector pET28a, which incorporates 6 × Histidine tags. Then, the constructed plasmid pET28a-*cyp168A1* was transferred into *E. coli* (BL21) for heterologous expression. The culture was induced by adding 0.6 mM isopropyl *β*-D-thiogalactopyranoside (IPTG) after the optical density at 600 nm (OD_{600}) reached 0.6 to 0.8. Then, the culture was incubated at 30°C for 10 h. *E. coli* was harvested by centrifuging at 4,000 rpm for 20 min, and the pellet was re-suspended with nickel column balance buffer (20 mM NaH_2PO_4-Na_2HPO_4, 300 mM NaCl, 10 mM imidazole, 6 M urea, pH 8.0); urea was used to denature the proteins to enhance solubility (26). The cell suspension was broken by repetitive sonication at 4°C, and the cell debris was removed by centrifugation at 10,000 rpm for 40 min. The his-CYP168A1 was loaded into the nickel column, and then washed by gradient imidazole buffers from 10, 40, 70, 100 to 300 mM (27). The residual

imidazole in the eluted buffer was removed by gradient dialysis from buffer I (20 mM KH_2PO_4-K_2HPO_4, 4 M urea, 5% glycerol, 1% glycine, 1‰ mercaptoethanol, pH 8.0) for 2 h, to buffer II (20 mM KH_2PO_4-K_2HPO_4, 2 M urea, 5% glycerol, 1% glycine, 1‰ mercaptoethanol, pH 8.0) for 2 h, and then to buffer III (20 mM KH_2PO_4-K_2HPO_4, 5% glycerol, 1% glycine, 1‰ mercaptoethanol, pH 8.0) for 3 h. CYP168A1 was successively refolded *in situ* through a gradient of decreased urea concentrations (26).

Western blot analysis and UV-vis characterization of purified CYP168A1. The purified CYP168A1 was determined by western blot analysis, using an anti-6 × His tag® antibody (Abcam, China). The purified CYP168A1 was diluted 10, 100, and 1,000 times, and 10 μL was transformed to PVDF film, respectively. The carbon monoxide (CO)-difference spectrum was performed in buffer (50 mM KH_2PO_4-K_2HPO_4, 1‰ mercaptoethanol, 5% glycerol, pH 8.0) at 20°C, respectively, in a 0.5-mL quartz cuvette with a 1-mm path length. Protein CYP168A1 was reduced by adding 10 mM dithionite, and the CO complex was performed by slow bubbling with CO gas for 1 min 30 s (27).

Construction of electron-supplying system and enzyme activity. To test the *in vitro* activity of CYP168A1, sufficient electrons must be supplied to the reaction system. Therefore, an electron-supplying system (named as FdFNR) was constructed by combining a 4Fe-4S ferredoxin (HS1040) (Fd) and a NAD(P)H-dependent ferredoxin reductase (HS6332) (FNR) with a glycine linker (GGGGG). The combined DNA

fragment was ligated to expression vector pETduet-1 at the second multiple cloning site (MCS). The protein was induced by adding 0.2 mM IPTG after the OD_{600} reached 0.6 to 0.8; then, the culture was incubated at 16°C for 10 h. Ultimately, the cells were broken in PBS buffer with the same method in the paragraph of CYP168A1 purification, and it was used as the electron-supplying cell free system. The electron supplying ability was determined with potassium ferricyanide ($K_3[Fe(CN)_6]$) as the receptor of the free donor, and NADPH as the source of donor. Absorbance of $K_3[Fe(CN)_6]$ at 340 nm was measured and the color feature (yellow) of $K_3[Fe(CN)_6]$ was captured. To test the enzyme activity of CYP168A1 with HBCDs, 1 mg/L HBCDs, 0.4 mM NADH, 5 μg purified CYP168A1 and 1 mL cell-free system were mixed, and the reaction system was incubated under different reaction conditions. The decrease in HBCD concentration was used to calculate enzyme activity. To test the effect of metal irons on enzyme activity, 10 mM chloride salts ($NiCl_2$, $CoCl_2$, $CaCl_2$, $CuCl_2$, $MnCl_2$, $ZnCl_2$, $MgCl_2$, KCl, $FeCl_2$ and $NaMoO_4$) were separately added to reaction system.

^{18}O isotope experiments and analysis. To confirm the source of the oxygen atom incorporated into the HBCD degradation products, $^{18}O_2$ and $H_2{}^{18}O$ were used to supply oxygen atoms for CYP168A1 reactions. The $^{18}O_2$ labeling reaction and anaerobic assay were performed in an anaerobic workstation AW200SG (Electrotek Ltd, UK). After excluding air for 1 h by N_2 atmosphere, all the liquid (1 mL FdFNR buffer, 5 μg purified CYP168A1) was exposed to an N_2 atmosphere for 30 min to

remove O_2. An activity assay system (equal to the system for enzyme activity detection) that was cell free containing enzyme and NADH was dried and dissolved in $H_2{}^{18}O$. All reactions were carried out at 30°C for 6 h. After terminating the reaction by adding 10 μL HCl (11.64 M) to the 1 mL reaction system, HBCDs were extracted by using an equal volume of ethyl acetate. Then, samples were mixed using vortex oscillation for 30 s. Before detection, the upper organic phase was concentrated 30 times. Samples were analyzed using ultra-high-performance liquid chromatography/time-of-flight mass spectrometry (UPLC-TOF/MS).

HBCDs or its products in activity assay experiments and the ^{18}O isotope experiments were quantified by UPLC-TOF/MS, equipped with an Eclipse XDB C18 analytical column (5 μm, 4.6 × 150 μm, Keystone Scientific, Agilent). HBCDs in samples used for products detection were extracted as the above described, and then, the organic phase was concentrated about 1,000 times. A mobile phase of water and methanol at a flow rate of 0.25 mL/min was applied for the target compounds. The proportional gradient of the mobile phase was started at 95% methanol, and increased linearly to 100% over 25 min, then decreased directly to 95% for 10 min. For mass spectrometric analysis, the ionization source was run in negative mode, and MS detection was set from 0 to 1,700 *m/z*. All target compounds were extracted based on their hydrogen adduct ions [M+H]- at *m/z* and characterization of bromine isotope (28).

Bromide detection. The detection of bromide was conducted on an ion

chromatograph coupled with an AS11-HC negative ion column (ICS-5000+, Thermo Fisher, Germany). The samples were prepared by terminating the reaction by adding 10 μL HCl to the 1 mL reaction system, followed by centrifugation at 12,000 rpm for 5 min to remove the proteins.

Gene deletion and complementation. The suicide vector pK18*mobsacB-Gm* used for gene deletion was derived from pK18*mobsacB* by replacing the kanamycin resistance gene with a gentamicin resistance gene (from plasmid pUCTn7T). Upstream (600 bp) and downstream (600 bp) fragments close to the target gene were amplified and aligned using fusion PCR, the primers and corresponding PCR functions used in this study were listed in Table 1. The constructed plasmid pK18*mobsacB-Gm-cyp168A1AB* was transferred from the *E. coli* donor strain S17-1 to *P. aeruginosa* HS9 by conjugal transfer. Donor strain S17-1 and recipient strain HS9 were mixed with a volume rate at 5:1 - 10:1 and cultured on LB solid media without antibiotics at 37°C for 4 h, and 30°C for 20 h, then the mixture was spread on M9 solid plates and incubated at 30°C for 48 h with 50 mg/L gentamicin, after it was resuspended and washed using saline solution. Finally, the correct transconjugants were washed and plated on LB-sucrose agar medium for plasmid elimination (29). The gene engineered groups were obtained by inserting a *lacZ* promoter with the genes *FdFNR* before *cyp168A1* (PLAC-HS9), or inserting a single *lacZ* promoter with the genes *FdFNR* followed *cyp168A1* (HS9-DW), or combined the operations of PLAC-HS9 and HS9-DW to get PLAC-DW. The *lacZ* promoter sequence was

amplified from clone vector pMD18T.

The expression vector pUC18k was used for gene complement in *P. aeruginosa*. The new expression plasmid pUC18k-*cyp168A1* was electrotransferred to strain HS9. Electrocompetent cells were prepared as follows: first, the strain was cultured in LB medium at 30°C after OD600 reached 0.6, and then the cells were pelleted at 4,000 rpm for 10 min, after incubating on ice for 20 min; finally, the cell pellets were washed twice using electroporation buffer (10% glycerol) (30). Correct transformants were verified by PCR and the cells were further incubated in LB medium with corresponding antibiotics.

Results

Genomic and proteomic profiles of strain HS9. Whole genome sequencing was preformed, and the sequence was assembled into a single circular chromosome without gaps (Fig. S1A). The circular chromosome is 6,876,988 bp in size, with a G + C content of 66.2% and 6,421 coding sequences (CDSs). Further analysis indicated that there were 157 CDSs annotated as related to metabolism of aromatic compounds (Fig. S1B). To explore functional genes involved in HBCD degradation, a proteomic analysis was carried out to compare the expression of proteins from cells incubated in the presence or absence of 1 mg/L HBCDs MSM media. A total of 1,770 proteins were identified, accounting for 27.6% of the genomic putative CDSs in strain HS9. Normalization was performed to average the abundance of all peptides. Differentially expressed proteins were filtered if their fold changes were over 2.0-fold with

significance > 20 (PEAKS Significance B Algorithm, p-value < 0.01) and if they had two unique peptides.

The expression of 277 proteins was significantly changed (≥ 2-fold change, *P*-value < 0.01), of which 190 proteins were up regulated and 87 were down-regulated (Fig. S1C). The up regulated proteins were divided into 25 categories by Clusters of Orthologous Groups (COGs) analysis (Fig. S1D). To narrow the search, the most significantly changed proteins (≥ 10-fold change, *P*-value < 0.01) are summarized in Fig. S2, and the HBCD-induced proteins are listed in Table S1. No annotated dehalogenases were identified among the 277 up regulated proteins, while the expression of the NADH reductase (HS5738), heme d1 biosynthesis protein (NirF) (HS1898) and iron (III) dicitrate transport protein (FecA) (HS1283) were up regulated with fold changes of 5.81, 217.80, and +∞, respectively. As many up regulated genes were related to electron donating, the functional genes that cooperated with electron donor were considered as possible HBCD degrading genes.

Many genes related to heavy metal were up regulated, including zinc and mercury transporting ATPase (EC 3.6.3.3), heavy metal sensor histidine kinase, copper resistance protein (CopC), Na^+/alanine symporter, iron (III) dicitrate transport protein (FecA), and zinc protease. Moreover, genes correlated with basic bioactivity, such as D-lactate dehydrogenase, L-lactate dehydrogenase (EC 1.1.2.3), L-lactate permease, and succinate dehydrogenase were significantly up regulated.

Identification of HBCD degrading genes. To identify the possible genes involved in

HBCD degradation in cooperation with Ferredoxin-NADP (+) reductase, three cytochrome P450 (CYP) proteins were selected as candidates. RT-qPCR assays were carried out to further detect the mRNA expression levels of the potential genes (Fig. 1A). The cytochrome P450 coding gene *cyp168A1* was up regulated in response to HBCDs with a fold change of 9.1. The HBCD consumption curve of strain HS9 was determined in a resting cell reaction system. The wild type of strain HS9 (WT) could degrade 1 mg/L HBCDs within 8 h. In addition, we also deleted or complemented the gene *cyp168A1*, and HBCD consumption capability of the mutant strain M*cyp168A1* was eliminated. When the *cyp168A1* gene was complemented in M*cyp168A1*, the HBCD degradation capability of strain W*cyp168A1* recovered to the same value as strain HS9 (Fig. 1B).

Verification of electron donor capability of cell free system-FdFNR. To confirm the donor supplying ability of FdFNR, potassium ferricyanide ($K_3[Fe(CN)_6]$) was used as the receptor of the free donor. Compared to the control group, the absorbance of $K_3[Fe(CN)_6]$ at A340 decreased to zero over 5 min, and the color feature (yellow) of $K_3[Fe(CN)_6]$ disappeared (Fig. 2A). Results showed that the cell free system was able to oxidize NADH to NAD^+ with an electron accepter present.

CYP168A1 is an efficient debromination enzyme. The gene *cyp168A1* was amplified and expressed in pET28a in *E. coli* BL21(DE3). The heterologously expressed 6 × His-CYP168A1 was successfully purified, with a molecular mass of 50

kDa (Fig. 2B), and the western blot analysis demonstrated the purified protein (Fig. S3A). The CO-difference spectrum showed that the purified protein has a strong absorbance at 450 nm (Fig. 2C). Results of enzyme activity detection showed that CYP168A1 degraded HBCDs in the presence of NADH in the FdFNR system. The optimal temperature for CYP168A1 activity was at 30°C (Fig. S3B), The effect of temperature on CYP168A1 stability was monitored by circular dichroism spectroscopy (CDS) (JASCO, Japan), which showed that CYP168A1 began to degenerate at temperatures above 35°C (Fig. S3C). Kinetic analysis revealed that the *Vmax* and *Km* were 0.73 U/mg and 0.35 mM (Fig. 2D), respectively. Most metal ions, including Ca^{2+}, Co^{2+}, Cu^{2+}, MoO_4^{2+}, enhanced enzyme activity, while Zn^{2+} and K^{+} did not (Fig. S3D).

Product analysis and ^{18}O isotope experiments. The products of the reaction catalyzed by CYP168A1 were identified using LC-TOF-MS, based on the mass spectra (*m/z*) of the target products. Products with molecular weights at $[M-H]^-$ 612.7000, 614.7000, and 616.7000, or 576.7240 and 578.7219 were detected. The results were matched to the previously reported standard compounds PBCDOHs and two tetrabromocyclododecadiols ($TBCDDOH_S$) (Fig. 3AB). Products with molecular weights at $[M-H]^-$ 450.8949, 388.9792, 325.0679 and 263.1655 were also detected (Fig. 3C-F). The bromide was detected by ion chromatography analysis (Fig. S4). These products suggest that CYP168A1 can degrade HBCDs through a debromination and hydrogenation process, and one oxygen atom was added to the product in each

322 step of the reaction. To determine the source of the oxygen that participates in the
323 reaction, ^{18}O isotope experiments were carried out as mentioned above. Products in
324 $^{18}O_2$ group had molecular weights of $[M-H]^-$ 611.5232, 612.6262, and 613.5282,
325 which match to PBCD^{16}OHs (Fig. 4A). In the ^{16}O-Not lyophilized and
326 ^{16}O-Lyophilized groups, PBCD^{16}OHs were detected (Fig. 4B, 4C). Thus,
327 lyophilization would not inactivate the enzyme activity. In contrast, products
328 containing ^{18}O, with molecular weights of $[M-H]^-$ 612.7000, 614.7000, 616.7000, and
329 617.4908, were only detected in the $H_2{}^{18}O$ group (Fig. 4D). Comparing the results of
330 Fig. 4A, B, and C with Fig. 4D, ^{18}O from $H_2{}^{18}O$ was added to PBCDOHs, and no ^{18}O
331 labeled products formed in the $^{18}O_2$ group. The results confirmed that the oxygen in
332 PBCD^{18}OHs was derived from $H_2{}^{18}O$. All the corresponding TIC spectrums for
333 products detection are shown in Fig. S5 and Fig. S6. The proposed pathway of HBCD
334 degradation catalyzed by CYP168A1 is shown in Fig. 5.
335
336 **Enhancement of degrading capacity of strain HS9.** To enhance the degrading
337 capacity of strain HS9, the expression of gene cyp168A1 and the combined donor
338 supplying system FdFNR were increased with a promoter lacZ was added as Fig. 6A.
339 The gene engineering modes and comparison of the HBCDs degrading ability of the
340 wild-type HS9 (WT), mutants PLAC-HS9, HS9-DW, and PLAC-DW are shown in
341 Fig. 6B. The cell growth and degrading rates of the mutants were detected in the
342 MSM-HBCDs system, and the results showed that the degrading rates of strain
343 HS9-DW were improved, compared to WT. However, increase the gene *cyp168A1*

expression cannot improve the degrading rate of HBCDs.

Phylogenetic analysis. Several amino acid sequences of dehalogenases CYPs, such as CYP7A11, CYP81A3v2 (17), CYP1A1, CYP2C11, CYP26B1 (13), CYP2E1 (15), CYP3A4 (17), CYP101 (14) and P450BM-1 (10), were compared, and the results showed that CYP168A1 was most closely related to CYP101 (Fig. 7).

Discussion

Hexabromocyclododecanes (HBCDs) have become a global research focus, due to their widespread pollution and serious harm to human health, such as inducing cancer (31), disrupting liver and thyroid hormones (32-33), and causing reproductive disorders (34). Several bacteria have been discovered from natural environments that can degrade HBCDs, such as *Pseudomonas* sp. HB01, *Bacillus* sp. HBCD-sjtu, *Achromobacter* sp. HBCD-1, *Achromobacter* sp. HBCD-2, and *P. aeruginosa* strain HS9 (35-38). Corresponding pathways have been proposed for these strains, but the specific molecular mechanisms of the degradation have not been revealed. In this study, the functional enzymes for HBCDs degradation from *P. aeruginosa* strain HS9 was characterized.

Proteomic analysis comparing the expression of proteins of the cells incubated was carried out with MSM medium in the presence or absence of 1 mg/L HBCDs, and the results showed that environmental stress response genes like lactate dehydrogenases (LDH) were up regulated in the HBCD group. *Enterococcus faecalis*

366 has general resistance to very different environmental stresses, depending on the
367 ability to maintain redox balance via LDH (39). In addition, decreases and increases
368 in salinity concentrations sharply increase the LDH activity of *Neanthes*
369 *arenaceodentata* (40). Moreover, succinate dehydrogenase was up regulated, which
370 could catalyze succinate to fumarate when a FADH was formed. Based on the above
371 information, we propose that the resistance of strain HS9 to HBCD stress occurs due
372 to maintaining the balance of reducing power in vivo, coupled with HBCD
373 degradation. HBCD could induce the expression of *cyp168A1* of strain HS9, while the
374 CYP168A1 cooperation with electron donators, and the electron transport and stress
375 resistance reactions (related to lactate dehydrogenases or succinate dehydrogenase)
376 were used to balance the electron supply in vivo.

377 In nature, cytochrome P450 (CYP) enzymes participate in degrading large
378 amounts of environmental pollutants. Typically, CYP monooxygenases introduce a
379 single oxygen atom into their substrates (41-43). However, there are few reports about
380 CYP enzymes simultaneously catalyzing debromination and hydrogenation reactions
381 (44). In this study, a novel CYP (CYP168A1) was shown to be the initial
382 dehalogenase enzyme in HBCD biodegradation. The gene *cyp168A1* was cloned and
383 expressed in *E. coli* and the enzymatic properties of the purified CYP168A1 were
384 investigated. The *Km* of CYP168A1 for HBCDs was 0.35 mM, while the *Km* of
385 γ-HBCD for LinB was 1.82 ± 0.60 μM, the affinity for HBCD to LinB is almost 1,000
386 times than that to CYP168A1. However, biochemistry information for the other two
387 major HBCD isomers to LinB was still limited. The affinity of CYP168A1 to HBCDs

was lower than that of LinA/B, it matched the lower degrading rate of strain HS9, compared to other HBCD degraders.

Considering the toxicity of HBCDs to the environment and humans, comparative metabolism studies and *in vitro* activity tests indicated that the human liver CYP3A4, maize CYPs, and male rat CYPs can degrade different HBCD isomers. To trace the source of gene *cyp168A1*, phylogenetic analysis was carried out. Several mono- and dihydroxylated metabolites of HBCDs are formed through catalyzing with the human liver CYP3A4, maize CYPs, and male rat CYPs, with mono-OH-HBCDs detected as the major metabolites (6, 17, 43). However, the products of HBCDs catalyzed by CYP168A1 were PBCDOHs and TBCDDOHs, generated from the debromination and hydrogenation processes of HBCDs, of which PBCDOHs were also identical to that produced by strain HS9 in HBCDs-MSM medium (21). This result revealed the difference of HBCDs biodegradation between eukaryotic cells and prokaryotic microorganisms.

In the reactions of 1,2-halododecanoic acids oxidation catalyzed by both CYP4A (44) and CYP52A (45), oxygen in 1,2-Hydroxydodecanoic acids derives from water, not from molecular oxygen, which was introduced by hydrolysis of an initially formed oxohalonium ($R–X^{+}–O^{-}$) metabolite. The results of ^{18}O isotope labeling reactions showed that H_2O serves as the source of the oxygen atom incorporated into PBCDOHs (Fig. 4). Mechanism of the oxygen addition was the same as oxidation of 1,2-halododecanoic acids by CYP4A and CYP52A. The present study revealed a novel mechanism of CYP to catalyze the brominated organic compounds.

In summary, this study reveals a new catalytic mechanism of CYP168A1 for the degradation of HBCDs, in which the debromination and hydrogenation reactions are carried out one after another. The ^{18}O isotope experiments show that the oxygen added into hydrated products were from H_2O. Engineering mutants of strain HS9 not only supplies new insights into biochemical properties of protein CYP168A1, but also serves as a model for enhancing the abilities of this strain in bioremediation.

Competing interests

All the authors declare no competing interests.

Authors' contributions

LH and HT outset and designed experiments. LH and WW performed experiments. HT and PX contributed reagents and materials. LH, HT, ZG, and PX wrote the paper. All Authors discussed and revised the manuscript. All Authors commented on the manuscript before submission. All authors read and approved the final manuscript.

Acknowledgements

This study was supported by the grants from National Key Research and Development Project (2018YFA0901200), from Shanghai Excellent Academic Leaders Program (20XD1421900), from 'Shuguang Program' (17SG09) supported by Shanghai Education Development Foundation and Shanghai Municipal Education Commission, from the National Natural Science Foundation of China (31770114),

and from the Science and Technology Commission of Shanghai Municipality (17JC1403300).

References

1. Fonseca VM, Jr VJF, Araujo AS, Carvalho LH, Souza AG. 2005. Effect of halogenated flame-retardant additives in the pyrolysis and thermal degradation of polyester sisal composites. *J Therm Anal Calorim* 79:429–433. https://link.springer.com/article/10.1007/s10973-005-0079-x
2. Tang H, Wang L, Wang W, Yu H, Zhang K, Yao Y, Xu P. 2013. Systematic unraveling of the unsolved pathway of nicotine degradation in *Pseudomonas*. *PLoS Genetics* 9: e1003923. https://www.ncbi.nlm.nih.gov/pubmed/24204321
3. Heeb NV, Wyss SA, Geueke B, Fleischmann T, Kohler HPE, Lienemann P. 2014. LinA2, a HCH-converting bacterial enzyme that dehydrohalogenates HBCDs. *Chemosphere* 107:194–202. DOI: 10.1016/j.chemosphere.2013.12.035
4. Heeb NV, Zindel D, Geueke B, Kohler HPE, Lienemann P. 2012. Biotransformation of hexabromocyclododecanes (HBCDs) with linB—an HCH-converting bacterial enzyme. *Environ Sci Technol* 46:6566–6574. DOI: 10.1021/es2046487
5. Heeb NV, Manuel M, Simon W, Birgit G, Hans-Peter EK, Peter L. 2018. Kinetics and stereochemistry of LinB-catalyzed δ-HBCD transformation: Comparison of in vitro and in silico results. *Chemosphere* 207:118–129. DOI: 10.1016/j.chemosphere.2018.05.057
6. Dimaano NG, Yamaguchi T, Fukunishi K, Tominaga T, Iwakami S. 2020. Functional characterization of cytochrome P450 CYP81A subfamily to disclose the pattern of cross-resistance in *Echinochloa phyllopogon*. *Plant Mol Biol*

102:403–416. DOI: 10.1007/s11103-019-00954-3

7. Ding J, Guotao LG, Huang Z. 2018. Research progress in microbial cytochrome P450 and xenobiotic metabolism. *Chinese J Appl Environ Biol* 3:657–662.

8. Karl F, Roger B. 2000. Cytochrome P4501A induction potencies of polycyclic aromatic hydrocarbons in a fish hepatoma cell line: Demonstration of additive interactions. *Environ Toxicol Chem* 19:2047–2058. https://setac.onlinelibrary.wiley.com/doi/10.1002/etc.5620190813

9. Brack W, Schirmer K, Kind T, Schrader S, Schüürmann G. 2010. Effect-directed fractionation and identification of cytochrome P4501 A-inducing halogenated aromatic hydrocarbons in a contaminated sediment. *Environ Toxicol Chem* 21:2654–2662. https://setac.onlinelibrary.wiley.com/doi/full/10.1002/etc.5620211218

10. Sakaki T, Yamamoto K, Ikushiro S. 2013. Possibility of application of cytochrome P450 to bioremediation of dioxins. *Biotechnol Appl Biochem* 60:65–70. https://www.ncbi.nlm.nih.gov/pubmed/23586993

11. Guo F, Iwakami S, Yamaguchi T, Uchino A, Sunohara Y, Matsumoto H. 2019. Role of CYP81A cytochrome P450s in clomazone metabolism in *Echinochloa phyllopogon*. *Plant Sci* 283:321–328. DOI: 10.1016/j.plantsci.2019.02.010

12. Iwakami S, Kamidate Y, Yamaguchi T, Ishizaka M, Endo M, Suda H, Nagai K, Sunohara Y, Toki S, Uchino A, Tominaga T, Matsumoto H. 2018. CYP81A P450s are involved in concomitant cross-resistance to ALS and ACCase herbicides in *Echinochloa phyllopogon*. *New Phytol* 221:2112–2122.

https://nph.onlinelibrary.wiley.com/doi/full/10.1111/nph.15552

13. Sakaki T, Shinkyo R, Takita T, Ohta M, Inouye K. 2002. Biodegradation of polychlorinated dibenzo-p-dioxins by recombinant yeast expressing rat CYP1A subfamily. *Arch Biochem Biophys* 401:0–98. https://www.ncbi.nlm.nih.gov/pubmed/12054491

14. Yan D, Liu H, Zhou NY. 2006. Conversion of *Sphingobium chlorophenolicum* ATCC 39723 to a hexachlorobenzene degrader by metabolic engineering. *Appl Environ Microbiol* 21:18. DOI: 10.1128/AEM.72.3.2283-2286.2006

15. Singh S, Sherkhane PD, Kale SP, Eapen S. 2011. Expression of a human cytochrome P450 2E1 in Nicotiana tabacum enhances tolerance and remediation of γ-hexachlorocyclohexane. *N Biotechnol* 28:423–429. DOI: 10.1016/j.nbt.2011.03.010

16. Huang H, Wang D, Wen B, Lv J, Zhang S. 2019. Roles of maize cytochrome P450 (CYP) enzymes in stereo-selective metabolism of hexabromocyclododecanes (HBCDs) as evidenced by in vitro degradation, biological response and in silico studies. *Sci Total Environ* 656:364–372. DOI: 10.1016/j.scitotenv.2018.11.351

17. Erratico C, Zheng X, Nele VDE, Tomy GT, Covaci A. 2016. Stereo-selective metabolism of α-, β- and γ-hexabromocyclododecanes (HBCDs) by human liver microsomes and CYP3A4. *Environ Sci Technol* 50:8263–8273. https://www.sciencedirect.com/science/article/pii/S1385894719312549

18. Esslinger S, Becker R, Maul R, Nehls I. 2011. Hexabromocyclododecane enantiomers: microsomal degradation and patterns of hydroxylated metabolites.

500 *Environ Sci Technol* 45:3938–3944. https://pubs.acs.org/doi/10.1021/es1039584
501 19. Zheng X, Erratico C, Abdallah MA, Negreira N, Luo X, Mai B, Covaci A. 2015.
502 In vitro metabolism of BDE-47, BDE-99, and *α*-, *β*-, *γ*-HBCD isomers by chicken
503 liver microsomes. *Environ Res* 143:221–228.
504 https://www.sciencedirect.com/science/article/pii/S0013935115301201
505 20. Zheng X, Erratico C, Luo X, Mai B, Covaci A. 2016. Oxidative metabolism of
506 BDE-47, BDE-99, and HBCDs by cat liver microsomes: implications of cats as
507 sentinel species to monitor human exposure to environmental pollutants.
508 *Chemosphere* 151:30–36. DOI: 10.1016/j.chemosphere.2016.02.054
509 21. Huang L, Wang W, Shah SB, Hu H, Xu P, Tang H. 2019. The HBCDs
510 biodegradation using a *Pseudomonas* strain and its application in soil
511 phytoremediation. *J Hazard Mater* 380:e120833.
512 https://www.sciencedirect.com/science/article/pii/S0304389419307861
513 22. Tang H, Yao Y, Zhang D, Meng X, Wang L, Yu H, Ma L, Xu P. 2011. A novel
514 NADH-dependent and FAD-containing hydroxylase is crucial for nicotine
515 degradation by *Pseudomonas putida*. *J Biol Chem* 286:39179–39187.
516 https://www.ncbi.nlm.nih.gov/pmc/articles/PMC3234743
517 23. Lu X, Wang W, Zhang L, Hu H, Xu P, Wei T, Tang H. 2019. Molecular
518 mechanism of *N, N*-Dimethylformamide degradation in a *Methylobacterium* sp.
519 strain DM1. *Appl Environ Microbiol* 85:e00275–319.
520 https://aem.asm.org/content/85/12/e00275-19
521 24. Yao X, Tao F, Zhang K, Tang H, Xu P. 2017. Multiple roles of two efflux pumps

522 in a polycyclic aromatic hydrocarbon-degrading, *Pseudomonas putida* strain B6-2
523 (DSM 28064). *Appl Environ Microbiol* 83:e01882-1917. DOI:
524 10.1128/AEM.01882-17
525 25. Yu H, Tang H, Zhu X, Li Y, Xu P. 2015. Molecular mechanism of nicotine
526 degradation by a newly isolated strain, *Ochrobactrum* sp. strain SJY1. *Appl*
527 *Environ Microbiol* 81:272–281. https://aem.asm.org/content/aem/81/1/272.full.pdf
528 26. Yu J, Zhang Y, Wang Z. 2018. Chicken (*Gallus gallus*) HNF1α expression in
529 *Escherichia coli* and its purification. *J Agricul Biotechnol* 3:e1.
530 27. Funhoff E G, Bauer U, Garcia-Rubio I, Beilen V J B. 2006. CYP153A6, a soluble
531 p450 oxygenase catalyzing terminal-alkane hydroxylation. *J Biol Chem* 188:
532 5220–5227. https://jb.asm.org/content/188/14/5220
533 28. Yu H, Hausinger RP, Tang H, Xu P. 2014. Mechanism of the
534 6-Hydroxy-3-succinoyl-pyridine 3-monooxygenase flavoprotein from
535 *Pseudomonas putida* S16. *J Biol Chem* 289:29158–29170. DOI:
536 10.1074/jbc.M114.558049
537 29. Qu Y, Ma Q, Liu Z, Wang W, Tang H, Zhou J, Xu P. 2017. Unveiling the
538 biotransformation mechanism of indole in a *Cupriavidus* sp. strain. *Mol Microbiol*
539 106:905–918. https://onlinelibrary.wiley.com/doi/full/10.1111/mmi.13852
540 30. Jiang Yi, Tang H, Wu G, Xu P. 2015. Functional identification of a novel gene,
541 *moaE*, for 3-Succinoylpyridine degradation in *Pseudomonas putida* S16. *Sci Rep*
542 5:13464. DOI: 10.1038/srep13464
543 31. Yvonne F, Inga B. 2009. Technical pentabromodipheny ether and

544 hexabromocyclododecane as activators of the pregnane-X-receptor (PXR).
545 *Toxicol*. 29:656−661. DOI: 10.1016/j.tox.2009.07.009
546 32. Palace VP, Pleskach K, Halldorson T, Danell R, Wautier K, Evans B. 2008.
547 Biotransformation enzymes and thyroid axis disruption in juvenile rainbow trout
548 (*Oncorhynchus mykiss*) exposed to hexabromocyclododecane diastereoisomers.
549 *Environ Sci Technol* 42:1967−1972. DOI: 10.1021/es702565h
550 33. Ven LTMVD, Verhoef A, Kuil TVD, Slob W, Leonards PEG, Visser TJ, Hamers T,
551 Herlin M, Hakansson H, Olausson H, Piersma A, Vos J. 2006. A 28-day oral dose
552 toxicity study enhanced to detect endocrine effects of hexabromocyclododecane in
553 Wistar rats. *Toxicol Sci* 94:281−292.
554 https://www.ncbi.nlm.nih.gov/pubmed/16984958
555 34. Makoto E, Sakiko F, Mutsuko H K, Mariko M. 2008. Two-generation
556 reproductive toxicity study of the flame retardant hexabromocyclododecane in rats.
557 *Reprod Toxicol* 25:335−351.
558 https://www.sciencedirect.com/science/article/abs/pii/S0890623807003383
559 35. Gao Y, Zhang X, Yang C. 2011. Photodegadation of hexabromocyclododecane in
560 water. *Environ Chem* 30:598−603.
561 36. Zhao YY, Zhang XH, Sojinu OS. 2010. Thermodynamics and photochemical
562 properties of alpha, beta, and gamma- hexabromocyclododecanes: a theoretical
563 study. *Chemosphere* 80:150−156. DOI: 10.1016/j.chemosphere.2010.04.002
564 37. Zhou D, Wu Y, Feng X, Chen Y, Wang Z, Tao T, Wei D. 2014. Photodegradation
565 of hexabromocyclododecane (HBCD) by Fe(III) complexes/H_2O_2 under simulated

566 sunlight. *Environ Sci Pollut Res* 21:6228–6233. DOI: 10.1007/s11356-014-2553-0
567 38. Nyholm J., Lundberg C, Andersson PL. 2010. Biodegradation kinetics of selected
568 brominated flame retardants in aerobic and anaerobic soil. *Environ Pollut*
569 158:2235−2240.
570 https://www.sciencedirect.com/science/article/pii/S0269749110000710
571 39. Rana NF, Sauvageot N, Laplace JM, Bao Y, Nes I, Rince A, Posteraro B,
572 Sanguinetti M, Hartke A. 2013. Redox balance via lactate dehydrogenase is
573 important for multiple stress resistance and virulence in *Enterococcus faecalis*.
574 *Infect Immun* 81:2662−2668. https://iai.asm.org/content/81/8/2662
575 40. Cripps RA, Reish DJ. 1973. The effect of environmental stress on the activity of
576 malate dehydrogenase and lactate dehydrogenase and lactate dehydrogenase in
577 *Neanthes arenacedentata* (Annelida: Polychaeta). *Comp Biochem Phys B*
578 46:123−133. DOI: 10.1016/0305-0491(73)90052-7
579 41. Durairaj P, Hur JS, Yun H. 2016. Versatile biocatalysis of fungal cytochrome
580 P450 monooxygenases. *Microb Cell Fact* 15:125.
581 https://www.ncbi.nlm.nih.gov/pmc/articles/PMC4950769
582 42. Urlacher VB, Girhard M. 2019. Cytochrome P450 monooxygenases in
583 biotechnology and synthetic biology. *Trends Biotechnol* 37:882–897.
584 https://www.sciencedirect.com/science/article/pii/S0167779919300010
585 43. Hakk H. 2016. Comparative metabolism studies of hexabromocyclododecane
586 (HBCD) diastereomers in male rats following a single oral dose. *Environ Sci*
587 *Technol* 50:89−96. https://pubs.acs.org/doi/10.1021/acs.est.5b04510

44. He X, Cryle MJ, De VJJ, Ortiz dMPR. 2005. Calibration of the channel that determines the ω-hydroxylation regiospecificity of cytochrome P4504A1. *J Biol Chem* 280: 22697–22705. DOI: 10.1074/jbc.M502632200

45. Kim D, Cryle MJ, De VJJ, Ortiz dMPR. 2007. Functional expression and characterization of cytochrome P450 52A21 from *Candida albicans*. *Arch Biochem Biophys* 464: 213–220.

Table 1. The primers used in this study. (The underline represents homologous sequences to the constructed vector)

Names	Sequence (3' - 5')	Function
GmF	CCCAAGCTTATGTTACGCAGCAGCAACGA	Replacement of resistance gene
GmR	CTAGCTAGCTTAGGTGGCGGTACTTGGGT	Replacement of resistance gene
Fcyp168A1	CCGGAATTCATGGACGACGCATTCAGCGA	Construction of pET28a-*cyp168A1*
Rcyp168A1	CCCAAGCTTCTCGCAGGTCTTCTGAGCGT	Construction of pET28a-*cyp168A1*
AFcyp168A1	TATGACATGATTACGAATTCATGGACGACGCATTCAGCGA	Gene knockout
ARcyp168A1	GTTATAAATTTGGAGTGTGAGCACGGCGTCGGGGCCGAAG	Gene knockout
BFcyp168A1	TCACACTCCAAATTTATAACGCGGCGAACGCGGTGGAGGA	Gene knockout
BRcyp168A1	AGGTCGACTCTAGAGGATCCCTCGCAGGTCTTCTGAGCGT	Gene knockout
Uplac-A1F	TGACATGATTACGAATTCCGAATACCAGAACCAGGGCA	Construction of PLAC-HS9/PLAC-DW
Uplac-A1R	TGAGTGAGCTAACTCACATTGGCCCTTGCTCCGCTGGGTT	Construction of PLAC-HS9/PLAC-DW
UplacF	AATGTGAGTTAGCTCACTCA	Construction of PLAC-HS9/PLAC-DW
UplacR	TCGCTGAATGCGTCGTCCATGGCGTAATCATGGTCATAGC	Construction of PLAC-HS9/PLAC-DW
Uplac-B1F	ATGGACGACGCATTCAGCGA	Construction of PLAC-HS9/PLAC-DW
Uplac-B1R	GCAGGTCGACTCTAGAGGATCC CCCGGCATCGCCGTGGCTGG	Construction of PLAC-HS9/PLAC-DW
Dplac-A2F	TGACATGATTACGAATTC CCAGCCACGGCGATGCCGGG	Construction of HS9-DW/PLAC-DW
Dplac-A2R	TGAGTGAGCTAACTCACATTCTACTCGCAGGTCTTCTGAG	Construction of HS9-DW/PLAC-DW
Dplac-F	AATGTGAGTTAGCTCACTCA	Construction of HS9-DW/PLAC-DW
Dplac-R	TCCAGCACGACGAAGGTCATGGCGTAATCATGGTCATAGC	Construction of HS9-DW/PLAC-DW
DFERF	ATGACCTTCGTCGTGCTGGA	Construction of HS9-DW/PLAC-DW
DFERR	GGCAGCCGGCTGATCCTGCGTCACTTCTCGACGAAGGCGC	Construction of HS9-DW/PLAC-DW
Dplac-B2F	CGCAGGATCAGCCGGCTGCC	Construction of HS9-DW/PLAC-DW
Dplac-B2R	GCAGGTCGACTCTAGAGGATCCGAGGCCGACGACTTCATGGA	Construction of HS9-DW/PLAC-DW
cyp168A1cF	GGTCGACTCTAGAGGATCCCATGGACGACGCATTCAGCGA	Gene complementation

cyp168A1cR	AGGTCGACTCTAGAGGATCCCTCGCAGGTCTTCTGAGCGT	Gene complementation

595 **Figure legends**

596 **Fig. 1. Identification of functional proteins.** (A) RT-qPCR verification of the
597 proposed functional genes in degrading HBCDs. In RT-qPCR assays, the treatment
598 group used HBCDs as the sole carbon source and the control group used sodium
599 citrate. HS651: putative cytochrome P450 hydroxylase; HS1037: cytochrome P450;
600 HS6073 (*cyp168A1*): putative cytochrome P450 hydroxylase (B) Comparison of the
601 HBCD degrading ability of the wild type HS9 (WT), *cyp168A1* deleted mutant strain
602 (M*cyp168A1*) and *cyp168A1* complemented strain (W*cyp168A1*).

603

604 **Fig. 2. Characterization of CYP168A1.** (A) Verification of the electron donor
605 capability of the cell free system-FdFNR. The protein expression of FdFNR was
606 measured and shown by SDS-PAGE, the color feature (yellow) of $K_3[Fe(CN)_6]$ was
607 captured, and the full wavelength scanning shows the concentration of $K_3[Fe(CN)_6]$ in
608 the cell free system. (B) SDS-PAGE analysis of CYP168A1. M: protein marker; lane
609 1, supernatant of the sonicated Bl21-pET28a-*cyp168A1*; lane 2, column effluent; lane
610 3, 10 mM imidazole buffer washed effluent; lane 4, 45 mM imidazole washed effluent;
611 lane 5, 70 mM imidazole washed effluent; lane 6, 100 mM imidazole washed effluent;
612 lane 7, 150 mM imidazole washed effluent. (C) The CO-difference spectrum of
613 CYP168A1. (D) Kinetic analysis of CYP168A1 (fitted to the Michaelis-Menten
614 kinetics).

615

616 **Fig. 3. Identification of intermediates of HBCD degradation by LC-TOF-MS.** (A)
617 Mass spectra of PBCDOHs. (B) Mass spectra of TBCDDOHs. (C)-(F) Corresponding

618 mass spectra of molecular weights (*m/z* 450.8949) (*m/z* 388.9792) (*m/z* 325.0679) and
619 (*m/z* 263.1655).
620
621 **Fig. 4. ^{18}O labeled products of HBCD degradation.** (A) Mass spectra extracted
622 from the ^{18}O group (PBCD^{16}OHs). (B) Mass spectra extracted from the ^{16}O-Not
623 lyophilized group (PBCD^{16}OHs). (C) Mass spectra extracted from the
624 ^{16}O-Lyophilized group (PBCD^{16}OHs). (D) Mass spectra extracted from the
625 ^{18}O-Lyophilized group (PBCD^{18}OHs).
626
627 **Fig. 5. Proposed pathway for HBCD degradation.** HBCDs were dehalogenated by
628 CYP168A1, with a serial of hydroxy added. The undetected oxohalonium metabolites
629 have been drawn in frame.
630
631 **Fig. 6.** Schematic for the gene engineering (A), and comparison of the HBCDs
632 degrading ability of the wild-type HS9 (WT) and genome edited mutants PLAC-HS9,
633 HS9-DW, and PLAC-DW (B).
634
635 **Fig. 7.** Phylogenetic tree analysis of CYP168A1 with reported cytochrome P450
636 enzymes that function in dehalogenation.

637 **Fig. 1**

638

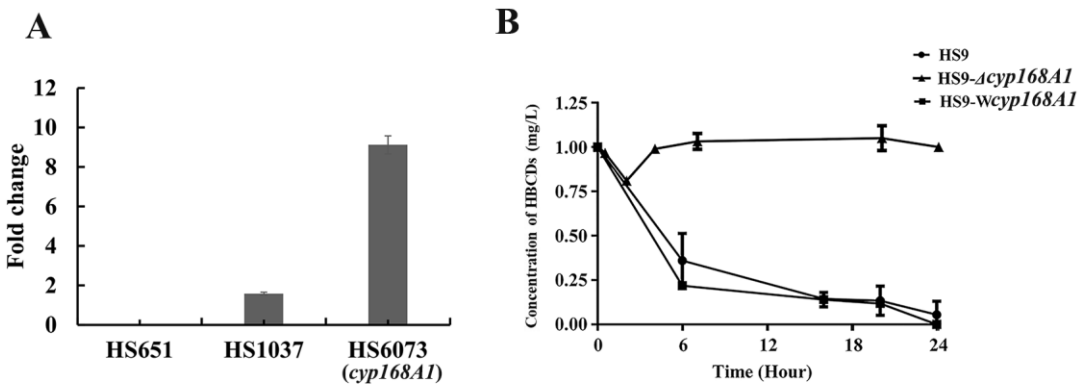

639

640 **Fig. 2**

641

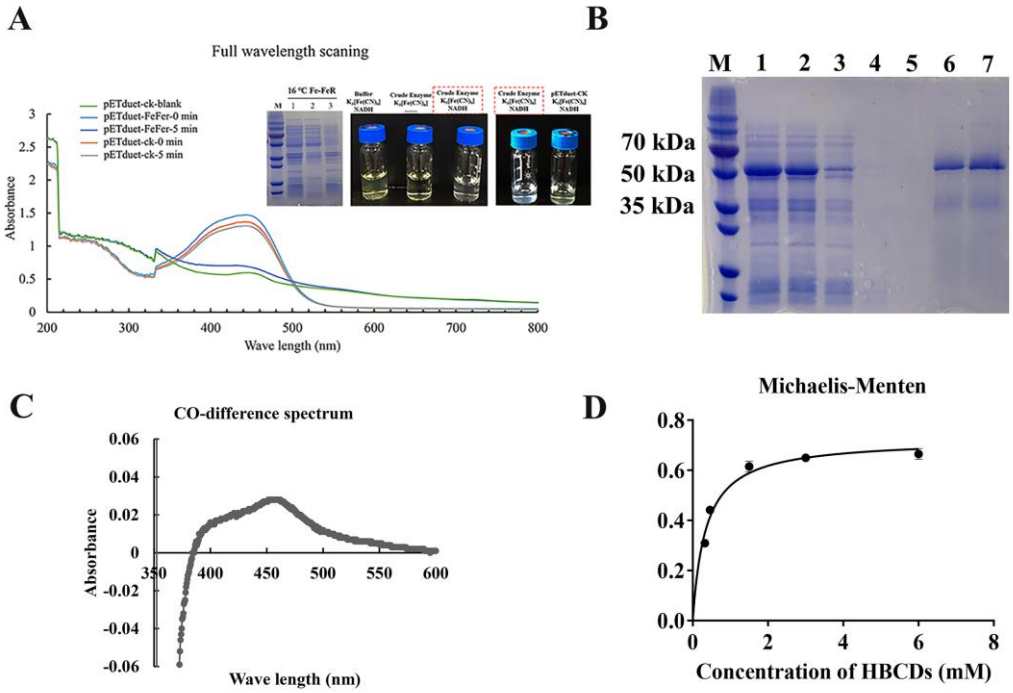

642

643 **Fig. 3**

644

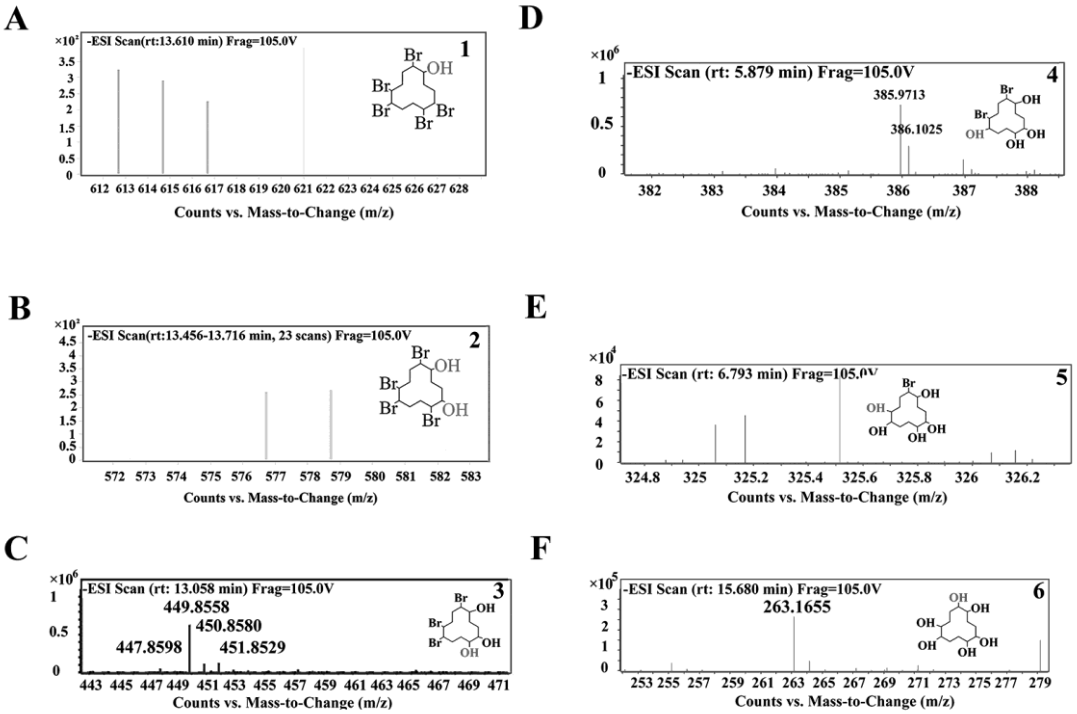

645

646 **Fig. 4**

647

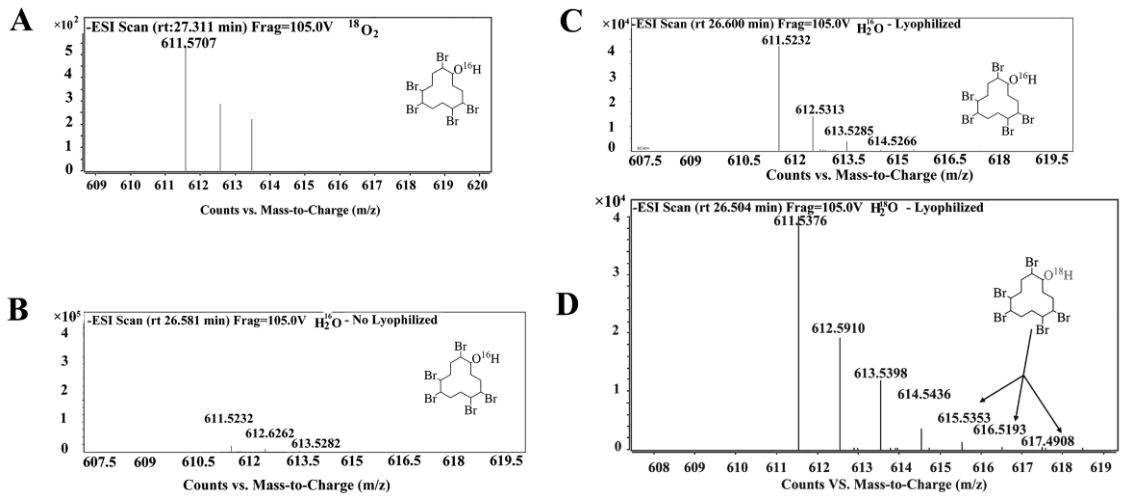

648

649 **Fig. 5**

650

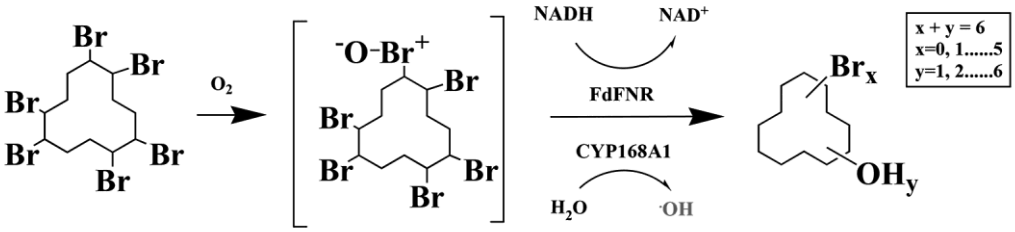

651

652 **Fig. 6**

653

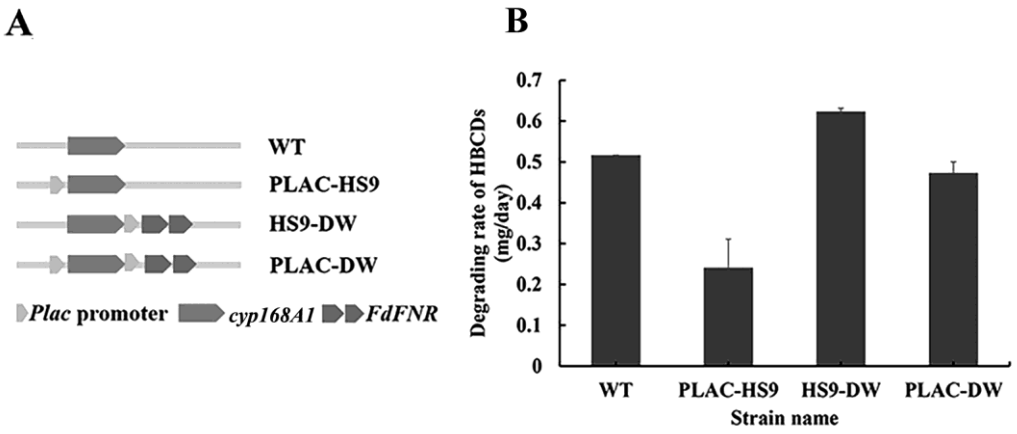

654

655 **Fig. 7**

656

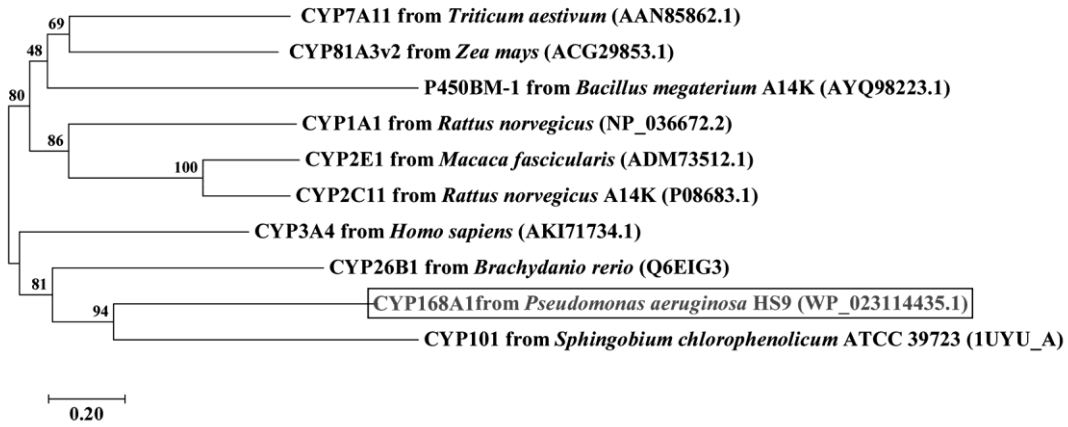

657